New Uniplanar Coplanar Waveguide Hybrid-Ring Couplers and Magic-T's

Chien-Hsun Ho, Lu Fan, and Kai Chang, *Fellow, IEEE*

Abstract— **The uniplanar coplanar waveguide (CPW) and slotline on a dielectric substrate have many applications to MIC and MMIC designs. A new reverse-phase CPW hybrid-ring coupler and a uniplanar CPW magic-T were developed. Experimental results showed that the hybrid-ring coupler has a 60% bandwidth centered at 3 GHz and the magic-T has a bandwidth of one octave from 2 to 4 GHz with 0.4 dB amplitude imbalance and 3.5° phase imbalance. Also, this paper presents theoretical analyses of CPW–slotline transitions using the transmission line models. Accurate modeling of nonuniform CPW and slotline radial stubs was developed using tandem connected uniform lines. Measured results of various CPW–slotline transitions agree very well with calculation. Design curves of the transitions are given for practical applications. To fully use the advantages of uniplanar structures, a 180° reverse-phase CPW–slotline back-to-back balun and a tee junction are described. Both circuits provide good amplitude and phase characteristic over a broad bandwidth due to the phase change of the circuits being independent of frequency.**

I. Introduction

ALTHOUGH microstrip is the most widely used planar transmission line, other forms of uniplanar transmission lines are available for circuit design. These uniplanar transmission lines include coplanar waveguide (CPW), slotline, and coplanar strip (CPS). Some drawbacks of using microstrip include sensitivity to substrate thickness, difficulty of inserting shunt solid-state devices, and the requirement of high-impedance lines for dc biasing. Uniplanar transmission lines have small dispersion, simple realization of short-circuited ends, the possibility of simple integration of lumped elements or active components, and circumventing the need for via holes. These characteristics make CPW, slotline, and CPS important in microwave and millimeter-wave integrated circuit design. Many attractive components using uniplanar structures have been published [1]–[6]. This paper presents uniplanar hybrid coupler components that have characteristics similar to those of the microstrip circuits, but with the advantages of uniplanar structure and better performance.

Manuscript received March 23, 1994; revised June 7, 1994. This work was supported in part by the U.S. Army Research Office, the NASA Center for Space Power, and the State of Texas Higher Education Coordinating Board's Advanced Technology Program.

C.-H. Ho was with the Department of Electrical Engineering, Texas A&M University, College Station, TX 77843 USA. He is now with Garmin Communication & Navigation, Lenexa, KS 66215 USA.

L. Fan and K. Chang are with Department of Electrical Engineering, Texas A&M University, College Station, TX 77843 USA.

IEEE Log Number 9405416.

To fully use the advantages of uniplanar structures, broad-band transitions of CPW–slotline are necessary. The theoretical analyses of CPW–slotline transitions using the transmission line models are presented in Section II. Simulations of various transitions agree very well with measurement results. Section III describes the fundamental characteristics of a 180° reverse-phase CPW–slotline balun and a tee junction. Both circuits use a 180° reverse-phase CPW–slotline back-to-back transition to achieve a 180° reversal. The phase shift of the circuits is frequency independent. In Sections IV and V, the designs and applications of a new reverse-phase CPW hybrid-ring coupler and a uniplanar CPW magic-T are illustrated. The circuit analyses for the CPW hybrids are based on simple transmission line circuit models. The measured results agree with the theoretical predictions very well.

II. Transmission Line Modeling of CPW–Slotline Transitions

Broad-band transitions from CPW to slotline [7]–[10] have been reported by many researchers. The transitions presented in [7], [8] use the CPW–slot double junction. The transitions in [9], [10] use the uniform slotline square stub and nonuniform slotline circular stub, respectively. In 1993, based on experimental investigations, the authors of this paper gave a systematic approach to this problem [11]. Various transitions were developed, and the best combination of using CPW short circuits and slotline radial stubs was proposed for broad-band matching between CPW and slotline. Based on the previous experimental investigations, this section presents an analysis of CPW–slotline transitions using simple equivalent circuit transmission line models on Touchstone. There is a fairly good agreement between measured and calculated results.

A. Uniform CPW–Slotline Transitions

The CPW–slotline transitions discussed here were fabricated on a 1.27-mm-thick RT/Duroid 6010 ($\epsilon_r = 10.8$) substrate. The CPW and slotline feed lines were both chosen as 50 Ω. Fig. 1 shows the circuit configuration and equivalent transmission line model of the uniform CPW–slotline cross-junction, which was defined as the type-a transition in {11}. The CPW and slotline in Fig. 1(a) cross each other at a right angle. The CPW extends one quarter-wavelength beyond the slotlines and terminates with an open circuit, while the slotline extends one quarter-wavelength beyond the CPW and terminates with a short circuit. The extensions of CPW and slotline act as a tuning stub to match each other. Fig. 2(a) shows the measured

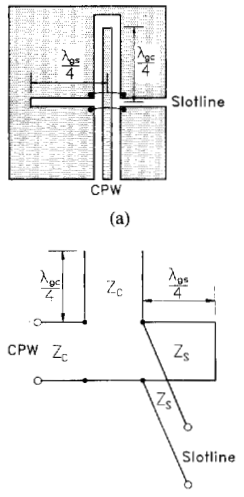

Fig. 1. (a) Physical configuration and (b) equivalent transmission line model for the type-a CPW–slotline transition.

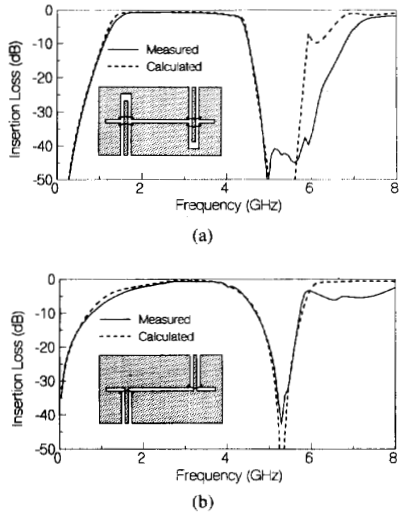

Fig. 2. Measured and calculated insertion loss of one pair of (a) type-a and (b) type-b CPW–slotline transitions. CPW gap size $G_C = 0.25$ mm, CPW center and conductor width $S_C = 0.5$ mm, slotline line width $W_S = 0.1$ mm, $\lambda_{gc} = 41.64$ mm, $\lambda_{gs} = 46.98$ mm.

and calculated frequency responses of insertion loss for the type-a back-to-back transition. The calculated results agree very well with the experimental data with less than 0.5 dB difference in the passband region. The bandwidth for insertion loss of less than 1 dB for the type-a back-to-back transition is from 1.6 to 3.6 GHz. The transition using a CPW short with a slotline $\lambda_{gs}/4$ shorted stub, i.e., type-b transition, is a special case of the uniform CPW–slotline cross junction. Fig. 2(b) shows the measured and calculated frequency responses of insertion loss for the type-b back-to-back transition. The type-b CPW–slotline transition has a narrow bandwidth because it depends only on a slotline $\lambda_{gs}/4$ shorted stub which is strongly frequency dependent.

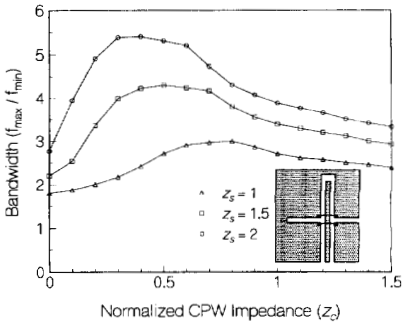

Fig. 3. Calculated 1 dB bandwidth of the type-a back-to-back transition against the normalized CPW characteristic impedance.

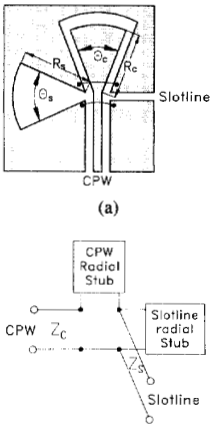

Fig. 4. (a) Physical configuration and (b) equivalent transmission line model for the type-h CPW–slotline transition.

For practical applications, it is useful to know the optimal combination of the CPW and slotline characteristic impedances. Fig. 3 shows the calculated 1 dB bandwidth of the uniform CPW–slotline back-to-back transition with given normalized slotline characteristic impedances $z_s = 1$, 1.5, and 2, against the normalized CPW characteristic impedance z_c. As shown in Fig. 3, it is noticeable that the optimum z_c for the maximum bandwidth decreases with the larger z_s. For $z_s =$ 1, 1.5, and 2, the optimum normalized CPW characteristic impedances are $z_c = 1$, 0.5, and 0.3, respectively. In Fig. 3, given a z_c, the 1 dB bandwidth increases with a larger z_s. This implies that the slotline matching stubs are the dominant factors in designing the type-a transitions. Although the slotline characteristic impedance can be chosen as high as possible to increase the bandwidth, the required optimum CPW characteristic impedance might be too low to be implemented.

B. Nonuniform CPW–Slotline Transitions

Fig. 4 shows the circuit configuration and equivalent transmission line model of the nonuniform CPW–slotline cross junction, which was defined as the type-h transition in [11].

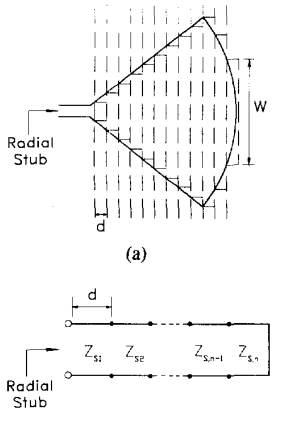

Fig. 5. (a) Radial stub modeled by tandem connected segments of piecewise uniform lines. (b) Equivalent transmission line model.

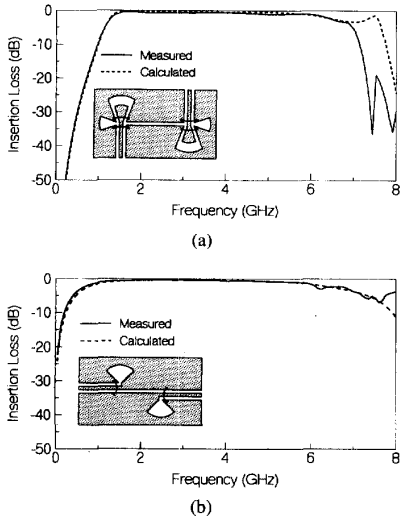

Fig. 6. Measured and calculated insertion loss of one pair of (a) type-h and (b) type-g CPW–slotline transitions. CPW feed line gap size $G_C = 0.25$ mm, center conductor width $S_C = 0.5$ mm, slotline feed line width $W_S = 0.1$ mm, $R_C = 6$ mm, $\theta_C = 60°$, $R_S = 6$ mm, and $\theta_S = 60°$.

The CPW and slotline radial stubs are used for broad-band impedance matching. They are modeled by tandem-connected segments of piecewise uniform lines, as shown in Fig. 5. Fig. 6(a) shows the measured and calculated frequency responses of insertion loss for the type-h back-to-back transition. The calculated results were obtained from the equivalent transmission line model of Fig. 4(b) with the radial stub simulated by a cascade of ten line segments of equal length but different characteristic impedance and dispersion characteristics. The theoretical results agree very well with the experimental data. The 1 dB bandwidth of the type-h transition is from 1.5 to 6.0 GHz. Similar modeling was carried out for a type-g CPW–slotline transition, and the results are given in Fig. 6(b). Type-g can be considered as the special case of

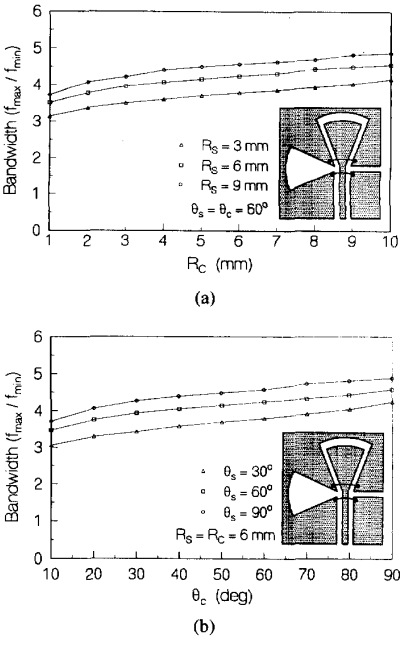

Fig. 7. Calculated 1 dB bandwidth of the type-h back-to-back transition against (a) the radius and (b) the angle of the CPW radial stub.

the nonuniform CPW–slotline cross junction. The CPW radial stubs are replaced by CPW shorts.

Fig. 7(a) shows the calculated 1 dB bandwidth with given radii of the slotline radial stub $R_S = 3$, 6, and 9 mm, against the radius of the CPW radius stub R_C. As shown in Fig. 7(a), the 1 dB bandwidth increases with a larger CPW radius because the larger CPW radial stub provides a better shorted circuit. Fig. 7(b) shows the calculated 1 dB bandwidth with given radial angles of the slotline radial stub $\theta_S = 30°$, 60°, and 90°, against the angle of the CPW radius stub θ_C. Again, the 1 dB bandwidth increases with a larger CPW radial stub.

As shown in Fig. 6, the type-g CPW–slotline transition has a broader bandwidth than the type-h CPW–slotline transition because the CPW short is an ideal short circuit and the slotline radial stub is a broad-band open. The bandwidth of the nonuniform transition with a CPW radial stub is always lower than that of the nonuniform transition with a CPW short.

III. 180° Reverse-Phase CPW–Slotline Baluns and Tee Junction

A. 180° Reverse-Phase CPW–Slotline Baluns

It is well known that a 180° phase change in excess of the signal path occurs when two microstrip-to-parallel-plate-line tapered baluns are connected back to back [12]. This phase change can be used in wide-band circuits. Hede [13] also presented a broad-band pulse inverter based on the same principle in 1977. The bandwidth measurement indicates that the pulse inverter works up to 1 GHz. Fig. 8(a) shows the 180° reverse-phase microstrip back-to-back tapered

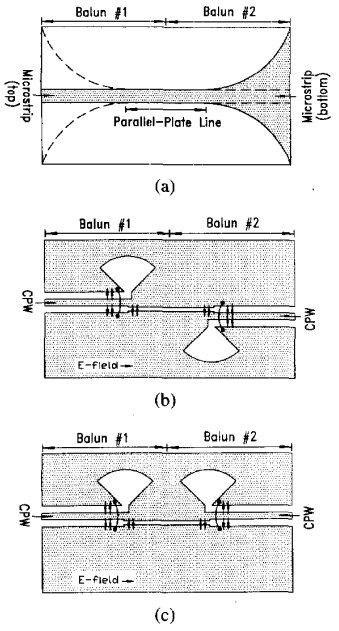

Fig. 8. Circuit configurations and schematic diagrams of E-field distribution for (a) the 180° reverse-phase microstrip back-to-back baluns, (b) the 180° reverse-phase CPW–slotline back-to-back baluns, and (c) the in-phase CPW–slotline back-to-back baluns.

baluns which are commonly used in the balanced mixers and antenna feeds. Although the 180° reverse-phase microstrip back-to-back tapered baluns have a very wide bandwidth, the use of double-sided ground planes results in a complicated fabrication and packaging process. To overcome this problem, a new uniplanar 180° reverse-phase back-to-back balun using two broad-band CPW–slotline transitions is described in the following.

Fig. 8(b) shows the circuit configuration and schematic diagram of E-field distribution for the 180° reverse-phase CPW–slotline back-to-back baluns. The two CPW–slotline transitions use CPW shorts and slotline radial stubs. The slotline radial stubs are placed on the opposite side of the internal slotline (i.e., a pair of type-g CPW–slotline transitions in [11]). Each side of the internal slotline connects the center conductor (or ground plane) of the CPW in balun 1 and the ground plane (or center conductor) of the CPW in balun 2. Referring to Fig. 8(b), a 180° phase change of the E field is introduced into the output signal at balun 2 when the input signal is excited from balun 1. The phase change of the E-field direction is caused by the inserted slotline section which connects the opposite sides of the CPW gaps at baluns 1 and 2. In Fig. 8(c), the in-phase CPW–slotline back-to-back baluns have two slotline radial stubs which are placed on the same side of the internal slotline section. The E-field directions of the CPW's are in phase at baluns 1 and 2.

To demonstrate the 180° phase reversal of the twisted CPW–slotline back-to-back baluns, a 180° reverse-phase and an in-phase CPW–slotline back-to-back balun were built. The test circuits were fabricated on a 1.27-mm-thick RT/Duroid 6010.8 ($\epsilon_r = 10.8$) substrate with the parameters: characteristic impedance of the CPW and slotline $Z_{C0} = 50\ \Omega$, $Z_S = 50\ \Omega$. The measurements were made using standard SMA connectors and an HP-8510 network analyzer. The measured insertion loss includes two coaxial–CPW transitions and two CPW–slotline transitions.

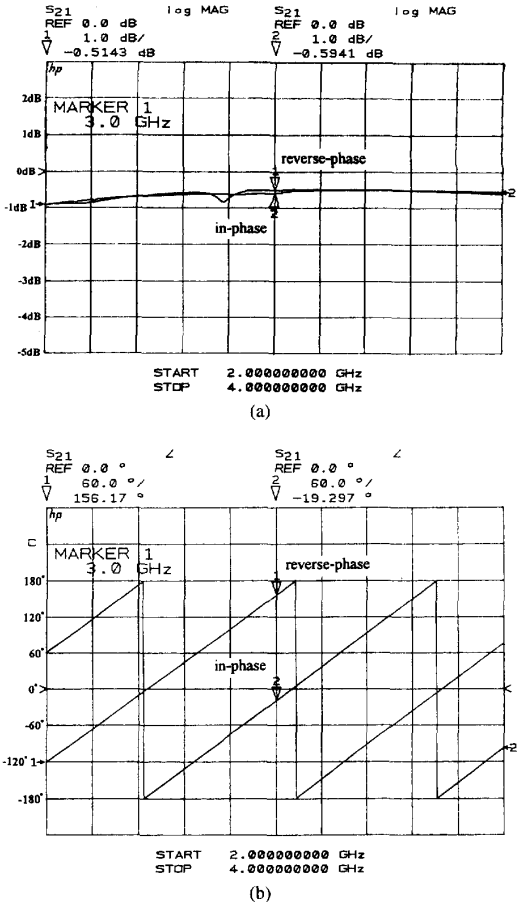

Fig. 9. Measured frequency responses of (a) insertion loss and (b) phase angle for the in-phase and 180° reverse-phase CPW–slotline back-to-back baluns.

Fig. 9(a) and (b) show the measured frequency responses of insertion loss and phase angle for the 180° reverse-phase and in-phase CPW back-to-back baluns, respectively. The amplitude difference between the 180° reverse-phase and in-phase CPW back-to-back baluns is within 0.3 dB from 2 to 4 GHz. Over the same range, maximum phase difference is maintained within 5°. The 5° phase error is due to the mechanical tolerances, misalignments, connectors, and discontinuities.

B. 180° Reverse-Phase CPW–Slotline Tee Junction

Fig. 10 shows the circuit configuration and schematic diagram of the E-field distribution for a 180° reverse-phase CPW–slotline tee junction. The circuit consists of one CPW–slotline tee junction and two CPW–slotline transitions. The arrows shown in Fig. 10 indicate the schematic expression of the electric field in the CPW's and slotlines. The E field in the input CPW (near the CPW–slotline tee junction) is

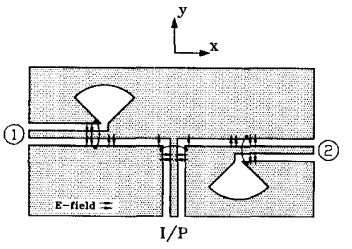

Fig. 10. Circuit configuration and schematic diagram of E-field distribution for the 180° reverse-phase CPW–slotline tee junction.

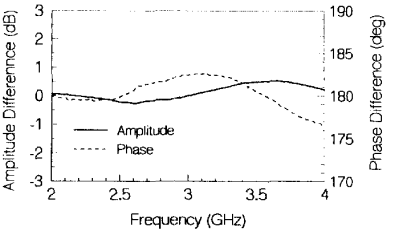

Fig. 11. Measured frequency responses of amplitude and phase differences for the uniplanar 180° reverse-phase CPW–slotline tee junction.

directed to the CPW center conductor. This produces two slotline waves with the E field in the $+y$ direction. At the transition of port 1, the $+y$-directed slotline E field will cause the E field in the output CPW to direct toward the CPW center conductor. However, the E field of the output CPW at port 2 will direct toward the CPW ground plane due to the $+y$-directed slotline E field.

According to the above principle, a truly 180° reverse-phase CPW–slotline tee junction was built on a 1.27-mm-thick RT/Duroid 6010.8 ($\epsilon_r = 10.8$) substrate with the parameters: characteristic impedance of the CPW feed lines $Z_{C0} = 50\ \Omega$, characteristic impedance of the slotline $Z_S = 70.7\ \Omega$. Fig. 11 shows the frequency responses of the amplitude and phase difference. The maximum amplitude difference is 0.6 dB from 2 to 4 GHz. Over the same frequency range, the maximum phase difference is 3.5°.

IV. 180° Reverse-Phase Hybrid-Ring Couplers

Hybrid couplers are indispensable components used in various MIC applications such as balanced mixers, balanced amplifiers, frequency discriminators, phase shifters, and feeding networks in antenna arrays. The rat-race hybrid-ring coupler [14] is the well-known and commonly used 180° hybrid. The 20–26% bandwidth of the rat-race coupler limits its applications to narrow-band circuits. Several design techniques have been developed to extend the bandwidth. One technique in [15], [16] used a $\lambda_g/4$ coupled-line section to replace the $3\lambda_g/4$ section of the conventional $3\lambda_g/2$ microstrip rat-race hybrid-ring coupler. Although the bandwidth of the reverse-phase hybrid-ring coupler has been improved up to more than one octave, the difficulty of constructing the shorted coupled-line section limits its use at low frequencies. In 1971, Chua [17] proposed a modified microstrip reverse-phase hybrid-ring coupler. The coupler substitutes a $\lambda_g/4$ slotline for the $3\lambda_g/4$ phase delay section of the conventional microstrip rat-race hybrid-ring coupler. Although the modified version gives good performance, the double-sided implementation of a curved $3\lambda_g/4$ microstrip line with an inserted $\lambda_g/4$ slotline is not easy for the photolithography process. Also, the ground pins are needed for the microstrip shorts.

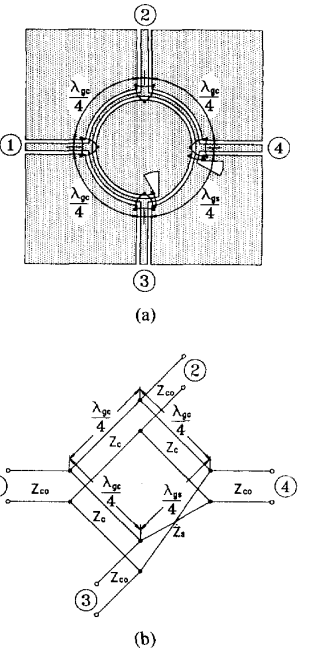

Fig. 12. (a) Circuit configuration and (b) equivalent transmission line model of the uniplanar reverse-phase hybrid-ring coupler.

To overcome these problems, this section reports a uniplanar reverse-phase CPW hybrid-ring coupler using a 180° reverse-phase CPW–slotline back-to-back balun. Since this 180° phase change of the CPW–slotline balun is frequency independent, the resulting uniplanar reverse-phase hybrid-ring coupler provides good amplitude and phase characteristics over a broad bandwidth. The experimental results agree very well with the theoretical design.

Fig. 12(a) shows the circuit layout of the uniplanar reverse-phase CPW hybrid-ring coupler. The circuit consists of four CPW–slotline tee junctions, three quarter-wavelength CPW sections, and one 180° reverse-phase CPW back-to-back balun. As shown in Fig. 12(a), the reverse-phase hybrid-ring coupler substitutes a 180° CPW–slotline phase shifter for the phase delay section used in the conventional rat-race hybrid-ring coupler. The resulting hybrid-ring coupler has a broad bandwidth because the phase change of the 180° reverse-phase CPW back-to-back balun is frequency independent. Fig. 12(b) shows the equivalent transmission line model. The twisted transmission line represents the 180° phase reversal of the CPW–slotline back-to-back baluns.

To test the circuit, a truly uniplanar reverse-phase hybrid-ring coupler was built on an RT/Duroid 6010.8 ($\epsilon_r = 10.8$) substrate with the following dimensions: substrate thickness $h = 1.524$ mm, characteristic impedance of the CPW feed lines $Z_{C0} = 50\ \Omega$, CPW feed lines center conductor width

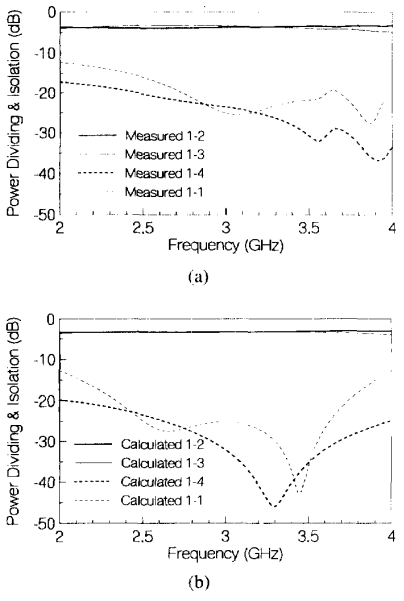

Fig. 13. (a) Measured and (b) calculated frequency responses of power dividing, return loss, and isolation for the uniplanar reverse-phase hybrid-ring coupler.

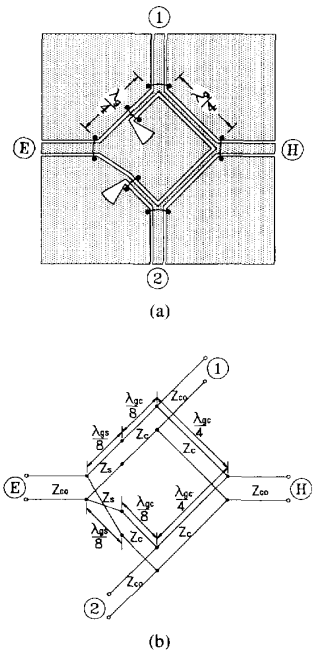

Fig. 14. The uniplanar magic-T (a) circuit configuration and (b) equivalent transmission line model.

$S_{C0} = 0.54$ mm, CPW feed lines gap size $G_{C0} = 0.3$ mm, characteristic impedance of the CPW ring $Z_C = 70.7\ \Omega$, CPW ring center conductor width $S_C = 0.27$ mm, CPW ring gap size $G_C = 0.5$ mm, characteristic impedance of the reverse-phase slotline section $Z_S = 70.7\ \Omega$, slotline line width $W_S = 0.47$ mm, radius of the slotline radial stub $r = 5$ mm, angle of the slotline radial stubs $\theta = 30°$, and CPW ring mean radius $r = 6.70$ mm. The measurements were made using standard SMA connectors and an HP-8510 network analyzer. A computer program based on the equivalent transmission mode of Fig. 12(b) was developed and used to analyze the circuit.

Fig. 13(a) and (b) show the measured and calculated frequency responses of power dividing, return loss, and isolation, respectively. The measured results show that the coupling of the power from port 1 to ports 2 and 3 is 3.4 and 3.7 dB at 3 GHz, respectively. The isolation is 23 dB at 3 GHz. A maximum amplitude imbalance of 0.9 dB has been achieved over a bandwidth from 2 to 3.6 GHz. The isolation between ports 1 and 4 is more than 17 dB over the bandwidth of 2–4 GHz. The calculated results agree very well with the experimental results. As expected, the power-dividing characteristics of the reverse-phase CPW hybrid-ring coupler is less frequency dependent. The insertion loss is mainly from the CPW–slotline transitions.

V. Uniplanar CPW Magic-T's

Magic-T's are fundamental components for many microwave circuits such as power combiners or dividers, balanced mixers, and frequency discriminators. The matched waveguide double-tee is a well-known and commonly used waveguide magic-T [18]. In 1964, [19] first proposed a planar magic-T. The circuit uses an asymmetric coupled transmission line directional coupler and Shiffman's phase-shift network. In 1965, [20] proposed a tapered-line magic-T. The circuit is based on a tapered asymmetrical transformer consisting of two coupled tapered lines. The complete analysis of tapered-line magic-T was discussed in [21]. Reference [22] proposed a planar magic-T using a microstrip balun in 1976. In 1980, [23] proposed a planar magic-T which is constructed with microstrip–slotline tee junctions and coupled slotlines. The planar magic-T uses a double-sided structure and has a bandwidth from 2 to 10 GHz. The two balanced arms of the planar magic-T are on the same side and they do not need the crossover connection.

In recent years, uniplanar transmission lines have emerged as alternatives to microstrip in planar microwave integrated circuits. The uniplanar microwave integrated circuits do not use the back side of the substrate, and allow easy series and shunt connections of passive and active solid-state devices. The use of the uniplanar structures circumvents the need for via holes and reduces processing complexity. In 1987, [24] proposed a uniplanar magic-T which uses three CPW–slotline tee junctions and a slotline tee junction. The in-phase CPW excitation is via an air bridge and the slotline tee junction is used as a phase inverter. The uniplanar magic-T has a narrow bandwidth. In 1993, a broad-band uniplanar magic-T was developed using crossover slotline ring structure [25], [26]. A broad-band microstrip coupled slotline ring coupler was also developed [27]. This section presents a novel uniplanar magic-T circuit using a 180° reverse-phase CPW–slotline junction and three CPW tee junctions. The circuit has the advantages of broad bandwidth and good performance.

Fig. 14(a) shows the circuit configuration of the new uniplanar CPW magic-T. The uniplanar magic-T consists of a 180°

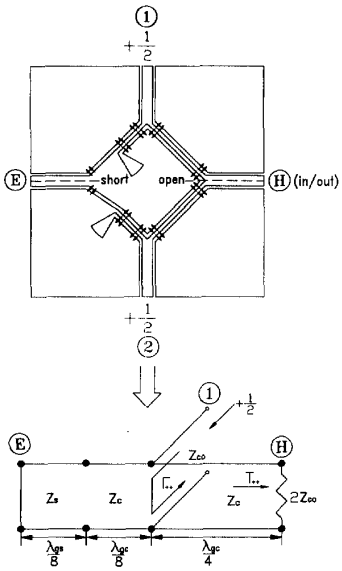

Fig. 15. Schematic expression of the electric field distribution and equivalent circuit for the in-phase coupling mode.

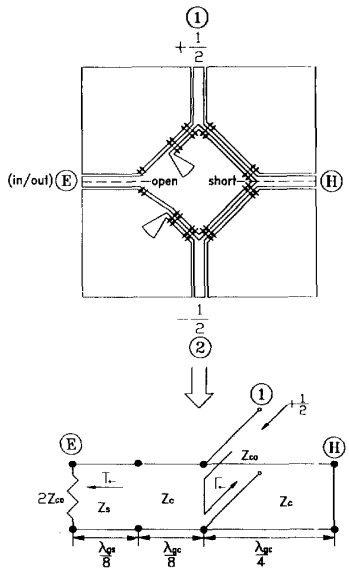

Fig. 16. Schematic expression of the electric field distribution and equivalent circuit for the 180° out-of-phase coupling mode.

reverse-phase CPW–slotline tee junction and three CPW tee junctions. The 180° reverse-phase CPW–slotline tee junction is used as a phase inverter. In Fig. 14(a), ports E and H correspond to the E and H arm of the conventional waveguide magic-T, respectively. Ports 1 and 2 are the power dividing balanced arms. Fig. 14(b) shows the equivalent transmission line model of the uniplanar CPW magic-T. The twisted transmission line in Fig. 14(b) represents the phase reversal of the CPW–slotline tee junction.

Figs. 15 and 16 show the schematic diagram of the E-field distribution and equivalent circuit for the in-phase and 180° out-of-phase couplings, respectively. The arrows shown in Figs. 15 and 16 indicate the schematic expression of the electric field in the CPW's and slotlines. In Fig. 15, the signal is fed to port H, and then divides into two components, which both arrive in phase at ports 1 and 2. The two component waves arrive at port E 180° out of phase and cancel each other. In this case, the symmetry plane at port H corresponds to an open circuit (magnetic wall), while the symmetry plane at port E corresponds to a short circuit (electric wall). In Fig. 16, the signal is fed to port E, and then divides into two components, which arrive at ports 1 and 2 with a 180° phase difference. The 180° phase difference between the divided signals at ports 1 and 2 is due to the 180° reverse-phase CPW–slotline tee junction. The two component waves arrive at port H 180° out of phase and cancel each other. The symmetry plane at port E corresponds to an open circuit (magnetic wall), whereas the symmetry plane at port H corresponds to a short circuit (electric wall). The isolation between ports E and H is perfect as long as the mode conversion in the reverse-phase CPW–slotline tee junction is ideal.

A two-port circuit calculation is used to analyze the isolation and impedance matching instead of the symmetric four-port networks because the circuit is symmetric with respect to ports E and H. The return loss at ports 1 and 2 is given by

$$|S_{11}|, |S_{22}| = \frac{1}{2}|\Gamma_{++} + \Gamma_{+-}| \tag{1}$$

where Γ_{++} and Γ_{+-} are the voltage reflection coefficients at port 1 for the in-phase mode coupling and 180° out of phase mode coupling, respectively. The isolation between ports 1 and 2 is given by

$$|S_{12}| = \frac{1}{2}|\Gamma_{++} - \Gamma_{+-}|. \tag{2}$$

To achieve the impedance matching at ports 1 and 2, i.e., $|S_{11}| = |S_{22}| = 0$, the characteristic impedance of CPW Z_C and slotline Z_S in terms of CPW feed line characteristic impedance Z_{C0} is given by

$$Z_S = Z_C = \sqrt{2}Z_{C0}. \tag{3}$$

According to (1)–(3), a truly uniplanar magic-T was built on a 1.524-mm-thick RT/Duroid 6010.8 ($\epsilon_r = 10.8$) substrate with the following dimensions: characteristic impedance of CPW feed lines $Z_{C0} = 50\ \Omega$, CPW feed lines center conductor width $S_{C0} = 0.54$ mm, CPW feed lines gap size $G_{C0} = 0.3$ mm, characteristic impedance of CPW in the magic-T $Z_C = 70.7\ \Omega$, magic-T's CPW center conductor width $S_C = 0.27$ mm, magic-T CPW gap size $G_C = 0.5$ mm, characteristic impedance of the slotline in the magic-T $Z_S = 70.7\ \Omega$, magic-T's slotline line width $W_S = 0.47$ mm, slotline radial stub angle $\theta = 30°$, and slotline radial stub radius $r = 5$ mm. The measurements were made using standard SMA connectors and an HP-8510 network analyzer. A computer program based on the equivalent transmission model of Fig. 14(b) was developed and used to analyze the circuit.

Fig. 17(a) shows the measured and calculated frequency responses of insertion loss for the H arm's power dividing (i.e., in-phase mode coupling). The extra insertion loss is less than 0.7 dB at the center frequency of 3 GHz. Similarly, Fig. 17(b)

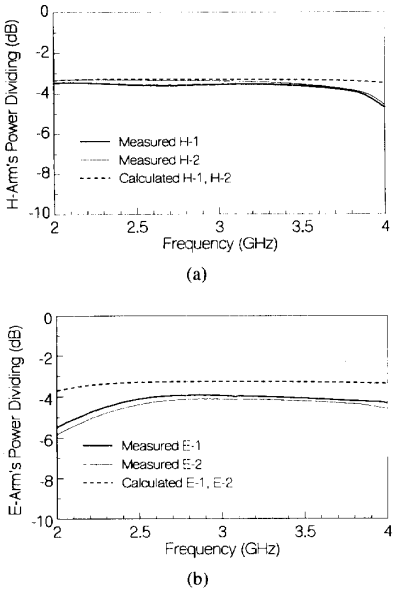

Fig. 17. Measured and calculated frequency responses of the magic-T (a) H arm's power dividing and (b) E arm's power dividing.

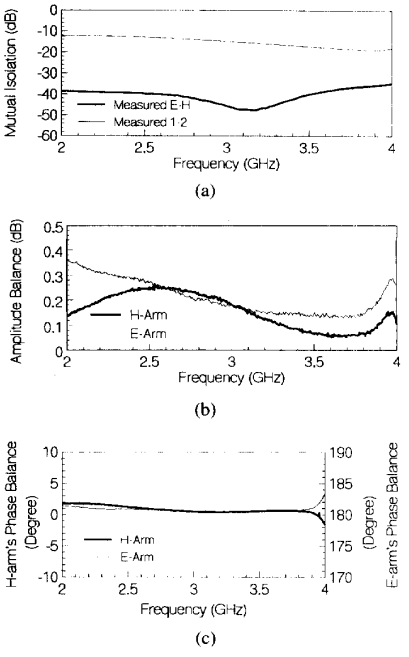

Fig. 18. Measured performance of the magic-T (a) isolation, (b) amplitude balance, and (c) phase balance.

shows the measured and calculated frequency responses of insertion loss for the E arm's power dividing (i.e., out-of-phase mode coupling). The insertion loss is less than 1.1 dB at the center frequency of 3 GHz. As shown in Fig. 17(a) and (b), the calculated results agree well with the measured results except the insertion loss. The additional insertion loss of the CPW magic-T in the measurement is mainly due to the CPW–slotline transition in the reverse-phase tee junction. As shown in Fig. 18, the isolation between the E and H arm is greater than 30 dB from 2 to 4 GHz. The mutual isolation between the two balanced arms is greater than 12 dB in the same frequency range. The H and E arm's maximum amplitude imbalances are 0.3 and 0.4 dB in the frequency range of 2–4 GHz, respectively. The H and E arm's maximum phase imbalance are 2° and 3.5° over the frequency range of 2–4 GHz, respectively.

VI. Conclusion

Simulations of CPW–slotline transitions using transmission line models were presented for the design applications of uniplanar structure. A simple and accurate modeling method for nonuniform CPW and slotline radial stubs using tandem-connected uniform lines have resulted in a very good agreement between simulation and measurement. A uniplanar 180° reverse-phase CPW–slotline balun and tee junction were demonstrated. The phase reversal of both circuits is frequency independent and can be applied to balanced circuits such as magic-T's and balanced mixers. A uniplanar magic-T and a reverse-phase hybrid-ring coupler were developed. The new uniplanar circuits use the combination of CPW's and slotlines on one side of the substrate. The uniplanar magic-T based on the principle of the 180° reverse-phase CPW–slotline tee junction demonstrated a bandwidth of one octave. The hybrid-ring coupler uses CPW–slotline back-to-back baluns to provide a 180° phase change which is independent of frequency. The reverse-phase CPW hybrid-ring coupler shows a fairly good performance over a 60% bandwidth. With the advantages of broad-band operation, simple design procedure, uniplanar structure, and ease of integrating with solid-state devices, these new uniplanar components should have many applications in microwave and millimeter-wave hybrid and monolithic integrated circuits.

References

[1] H. Ogawa and A. Minagawa, "Uniplanar MIC balanced multiplier—a proposed new structure for MIC's," *IEEE Trans. Microwave Theory Tech.*, vol. MTT-35, pp. 1363–1368, Dec. 1987.

[2] M. Abdo Tuko and I. Wolff, "Novel 36 GHz GaAsfrequency doublers using (M)MIC coplanar technology," in *IEEE MTT-S Int. Microwave Symp. Dig.*, June 1992, pp. 1167–1170.

[3] Y. H. Shu, J. A. Navarro, and K. Chang, "Electronically switchable and tunable coplanar waveguide-slotline band-pass filters," *IEEE Trans. Microwave Theory Tech.*, vol. 39, pp. 548–554, Mar. 1991.

[4] C. H. Ho, L. Fan, and K. Chang, "Broad-band uniplanar hybrid-ring coupler," *Electron. Lett.*, vol. 29, pp. 44–45, Jan. 1993.

[5] D. Cahana, "A new coplanar waveguide/slotline double-balanced mixer," in *IEEE MTT-S Int. Microwave Symp. Dig.*, 1989, pp. 967–968.

[6] T. Hirota and H. Ogawa, "Unipolar monolithic frequency doublers," *IEEE Trans. Microwave Theory Tech.*, vol. 37, pp. 1249–1254, Aug. 1989.

[7] W. Grammar and K. Yngvesson, "Coplanar waveguide transitions to slotline: Design and microprobe characterization," *IEEE Trans. Microwave Theory Tech.*, vol. 41, pp. 1653–1658, Sept. 1993.

[8] V. Trifunovic and B. Jokanovic, "New uniplanar balun," *Electron. Lett.*, vol. 27, pp. 813–815, May 1991.

[9] H. Fouad and L. Ramboz, "Broadband planar coplanar waveguide-slotline transition," in *1982 European Microwave Conf. Dig.*, pp. 628–631.

[10] T. Q. Ho and S. M. Hart, "A novel broad band coplanar waveguide to slotline transition," *IEEE Microwave Guided Wave Lett.*, vol. 2, pp. 415–416, Oct. 1992.

[11] C. H. Ho, L. Fan, and K. Chang, "Experimental investigations of CPW-slotline transitions for uniplanar microwave integrated circuits," in *IEEE MTT-S Int. Symp. Dig.*, June 1993, pp. 877–880.
[12] J. W. Duncan and V. P. Minerva, "100:1 bandwidth balun transformer," *Proc. IRE*, vol. 48, pp. 156–164, Jan. 1960.
[13] C. Hede, "High speed logic, Part 3," Tech. Rep. IR 127, Electromagnetics Inst., Technical Univ. Denmark, 1977.
[14] C. Y. Pon, "Hybrid-ring directional couplers for arbitrary power division," *IRE Trans. Microwave Theory Tech.*, vol. MTT-9, pp. 529–535, Nov. 1961.
[15] S. J. Robinson, "Broad-band hybrid junctions," *IRE Trans. Microwave Theory Tech.*, vol. MTT-8, pp. 671–672, Nov. 1960.
[16] S. March, "A wide band stripline hybrid ring," *IEEE Trans. Microwave Theory Tech.*, vol. MTT-16, p. 361, June 1968.
[17] L. W. Chua, "New broad-band matched hybrids for microwave integrated circuits," in *1971 Proc. European Microwave Conf.*, pp. C4/5:1–C4/5:4.
[18] K. Chang, *Handbook of Microwave and Optical Components, Vol. 1.* New York: Wiley, 1990, pp. 153–154.
[19] D. I. Kraker, "Asymmetric coupled-transmission-line magic-T," *IEEE Trans. Microwave Theory Tech.*, vol. MTT-12, pp. 595–597, Nov. 1964.
[20] R. H. DuHamel and M. E. Armstrong, "The tapered-line magic-T," in *Proc. 15th Annu. Symp. Dig. USAF Antenna Res. Program*, Monticello, IL, Oct. 1965, pp. 387–388.
[21] C. P. Tresselt, "Design and computed theoretical performance of three classes of equal-ripple non-uniform line couplers," *IEEE Trans. Microwave Theory Tech.*, vol. MTT-17, pp. 218–230, Apr. 1969.
[22] G. J. Laughlin, "A new impedance-matched wideband balun and magic-T," *IEEE Trans. Microwave Theory Tech.*, vol. MTT-24, pp. 135–141, Mar. 1976.
[23] M. Aikawa and H. Ogawa, "A new MIC magic-T using coupled slot lines," *IEEE Trans. Microwave Theory Tech.*, vol. MTT-28, pp. 523–528, June 1980.
[24] T. Hirota, Y. Tarusawa, and H. Ogawa, "Uniplanar MMIC hybrids—A proposed new MMIC structure," *IEEE Trans. Microwave Theory Tech.*, vol. MTT-35, pp. 576–581, June 1987.
[25] C. H. Ho, L. Fan, and K. Chang, "A broad-band uniplanar slotline hybrid ring coupler with over one octave bandwidth," in *IEEE MTT-S Int. Microwave Symp. Dig.*, June 1993, pp. 585–588.
[26] ——, "Broad-band uniplanar hybrid-ring and branch-line couplers," *IEEE Trans. Microwave Theory Tech.*, vol. 41, pp. 2116–2125, Dec. 1993.
[27] ——, "Slotline annual ring element and their applications to resonator, filter, and coupler design," *IEEE Trans. Microwave Theory Tech.*, vol. 41, pp. 1648–1650, Sept. 1993.

Chien-Hsun Ho, for a photograph and biography, see page 51 of the January issue of this TRANSACTIONS.

Lu Fan, for a photograph and biography, see page 51 of the January issue of this TRANSACTIONS.

Kai Chang (S'75–M'76–SM'85–F'91), for a photograph and biography, see page 51 of the January issue of this TRANSACTIONS.